Published in final edited form as:
Mol Cancer Ther. 2015 February ; 14(2): 499–512. doi:10.1158/1535-7163.MCT-14-0073.

Tumor suppressor role of Notch3 in Medullary Thyroid Carcinoma revealed by genetic and pharmacological induction

Renata Jaskula-Sztul[1], **Jacob Eide**[1,*], **Sara Tesfazghi**[1], **Ajitha Dammalapati**[1], **April D. Harrison**[1], **Xiao-Min Yu**[1], **Casi Scheinebeck**[2], **Gabrielle Winston-McPherson**[2], **Kevin R. Kupcho**[3], **Matthew B. Robers**[3], **Amrit K. Hundal**[1], **Weiping Tang**[2], and **Herbert Chen**[1]

[1]University of Wisconsin Medical School, Department of Surgery, University of Wisconsin

[2]School of Pharmacy and Department of Chemistry, University of Wisconsin

[3]Promega Corporation, Madison, WI

Abstract

Notch1-3 are transmembrane receptors that appear to be absent in Medullary Thyroid Cancer (MTC). Previous research has shown that induction of Notch1 has a tumor suppressor effect in MTC cell lines, but little is known about the biological consequences of Notch3 activation for the progression of the disease. We elucidate the role of Notch3 in MTC by genetic (doxycycline inducible Notch3 intracellular domain) and pharmacological (AB3, novel HDAC inhibitor) approaches. We find that overexpression of Notch3 leads to the dose dependent reduction of neuroendocrine tumor markers. In addition, Notch3 activity is required to suppress MTC cell proliferation, and the extent of growth repression depends on the amount of Notch3 protein expressed. Moreover, activation of Notch3 induces apoptosis. The translational significance of this finding is highlighted by our observation that MTC tumors lack active Notch3 protein and reinstitution of this isoform could be a therapeutic strategy to treat patients with MTC. We demonstrate, for the first time, that overexpression of Notch3 in MTC cells can alter malignant neuroendocrine phenotype in both *in vitro* and *in vivo* models. In addition, our study provides a strong rationale for using Notch3 as a therapeutic target to provide novel pharmacological treatment options for MTC.

Keywords

Notch3; tumor suppressor; medullary thyroid cancer (MTC); apoptosis; HDAC inhibitors

Corresponding authors:Herbert Chen, University of Wisconsin Medical School, Department of Surgery, 600 Highland Ave, BX 7375 Clinical Science Cntr, Madison, WI 53792-3284. Phone: 608-263-1387; Fax: 608-252-0912; chen@surgery.wisc.edu; and **Weiping Tang**, School of Pharmacy and Department of Chemistry, 7125 Rennebohm Hall, University of Wisconsin, Madison, WI 53705-2222. Phone: 608-890-1846; wtang@pharmacy.wisc.edu.
*Current Address: University of Minnesota, Medical School, 2221 University Ave SE #305, Minneapolis, Minnesota.

All financial disclosures:
There are no financial disclosures from any authors.

Disclosure of Potential Conflicts of Interest
No potential conflicts of interest were disclosed

Introduction

Medullary thyroid cancer (MTC) is a neuroendocrine (NE) tumor derived from the calcitonin-producing thyroid C-cells and accounts for 3–5% of all thyroid cancer cases (1–3). Although MTC is relatively uncommon, it disproportionally accounts for more than 14% of thyroid cancer related deaths. Complete surgical resection at a relatively early stage of the disease remains the only potential cure for MTC (3). Despite initial aggressive surgery, more than 50% of patients with MTC will have persistent disease, manifested as elevated postoperative calcitonin levels (4). Unlike liver metastases from other solid tumors which tend to develop as isolated and potentially resectable lesions, MTC liver metastases are almost always small and widely distributed throughout the liver, precluding curative surgical resection (5). Unfortunately, there is no curative therapy for patients with MTC liver metastases and/or widely metastatic disease (6,7). Although newer compounds have shown some activity in clinical trials, their affect on long-term survival has not been demonstrated (8,9). Moreover, there are no effective options to treat many of the debilitating symptoms associated with incurable MTC such as airway obstruction, flushing, abdominal pain, and diarrhea. While we and others have previously shown that resection of selected MTC tumor foci can provide temporary palliation (5), tumor progression inevitably leads to recurrence of the disabling symptoms. Therefore, understanding the molecular pathways involved in MTC progression is critical to develop effective treatments to improve local/regional control of MTC after surgery, as well as to treat distant metastatic disease.

The biochemical diagnosis of MTC is established by elevated levels of hormones secreted by C cells which include calcitonin, chromogranin A (CgA), and synaptophysin (SYP) (2,10). In addition, the basic helix-loop-helix transcription factor, achaete-scute complex-like 1 (ASCL1) is also highly expressed in MTC cells (11,12). Previous research has shown that ASCL1 is critical for the development of C cells and promoting MTC tumor growth (12,13). Moreover, this transcription factor supports the growth and survival of embryologic precursors by inhibiting apoptosis (14). It has been shown that ASCL1 is regulated by the Notch pathway on the transcriptional level (15,16) as well as by direct proteasomal degradation (17). It is apparent that MTC cell growth and NE tumor marker expression are governed by the same signaling pathway (13,18). The Notch signaling network is implicated in diverse functions during development, ranging from cell differentiation, cell proliferation, cell survival, and apoptosis (19,20). Notch mammalian proteins consist of four structurally related receptors Notch1-4 that interact with one of the ligands encoded by the Delta/Jagged gene families (*DLL1, DLL3, DLL4, JAG1, and JAG2*) (21). Ligand-receptor binding triggers pathway activation by inducing two proteolytic cleavages mediated by metalloprotease and γ-secretase, which release the Notch intracellular domain (NICD) to the nucleus. NICD forms a transcriptional activation complex with DNA binding transcription factor CSL (also called CBF-1, RBP-jk, Lag-1), the co-activator Mastermind-like (MAML), and other proteins (22) which subsequently induce expression of Hairy/Enhancer of Split (HES) and Hairy-related (HEY) transcriptional repressors (23). This canonical signaling cascade NICD-CBF1-HES/HEY, in turn, directly antagonizes expression of ASCL1.

In this paper, we demonstrate for the first time that Notch3 pathway activation contributes to the alteration of malignant phenotype in thyroid carcinomas of neuroendocrine origin. Our

results show that Notch3 protein is not expressed in human MTC tumor samples and cells. To elucidate the role of Notch3 expression we created a gain-of-function model by generating MTC cells with a doxycycline-inducible Notch3 intracellular domain. We further validated Notch3 antitumor properties in MTC cell lines by using novel class I HDAC inhibitor, AB3, which specifically induces Notch3. In our previous studies, compounds closely related to AB3 were identified as potent inhibitors for HDAC2 and HDAC3 (24). We show that forced Notch3 expression in MTC cell lines does not promote and indeed inhibits tumor cell proliferation by triggering apoptotic events in a dose dependent fashion. Importantly, Notch3 induction leads to the functional activation of Notch3 mediator CBF1, followed by changes in transcriptional levels of HES and HEY genes. Moreover, Notch3 activation causes a reduction in NET markers: ASCL1, CgA, SYP, and calcitonin indicating that this pathway is conserved in MTC. We also verify that Notch3 activity is required to reduce the growth rate of MTC-TT xenografts. Taken together, this study documents the tumor suppressing role of Notch3 in MTC in both *in vitro* and *in vivo* models, providing the rationale for targeting Notch3 with small molecule compounds to treat patients with MTC and other tumors in which this pathway is not active.

Materials and Methods

Cell culture

Human MTC cell line TT was kindly provided by Dr. Barry D. Nelkin (John Hopkins University, Baltimore, MD) in 2011and MZ-CRC-1 cell line was kindly provided by Dr. Gilbert Cote (MD Anderson Cancer Center, Houston, TX) in 2012. The control cell lines MIA-PaCa-2 and OVCAR-3 were obtained from ATCC in 2010 and 2009, respectively. Nontumorigenic human thyroid epithelial cell lines HTori-3 and Nthy-ori 3-1 were purchased from Sigma-Aldrich (partnership with the European Collection of Cell Cultures - ECACC) in 2011. The identity of cell lines were confirmed by short tandem repeat (STR) profile testing and the genotype of the cell lines is available in the American Type Culture Collection (ATCC) STR database and European Collection of Cell Cultures - ECACC. TT cells were maintained in RPMI 1640 medium (Life Technologies) supplemented with 16% fetal bovine serum (Sigma) and MZ-CRC-1 cells were maintained in DMEM/F-12 medium (Life Technologies) supplemented with 10% fetal bovine serum (Sigma). Both media were suplimented with 100 IU/mL penicillin (Invitrogen) and 100 μg/mL streptomycin (Invitrogen) in a humidified atmosphere of 5% CO2 in air at 37°C (25). Doxycycline inducible cell lines, TT-TRE NICD3, and TT-TRE (vector alone), were maintained in similar media to TT cells, except with tetracycline-free fetal bovine serum (Clontech), 75 μg/ml G418 (HyClone), and 50 μg/ml hygromycin (Invitrogen).

Human tissue samples

Human MTC tumor samples were obtained from Dr. Jeffrey Moley (Washington University, St. Louis, MO) and other control tumor samples were obtained from the University of Wisconsin Comprehensive Cancer Center Translational Science BioBank with known specimen pathology statuses. All tumor samples were snap frozen in liquid nitrogen and stored in −80°C. Tumor cell lysates were prepared for Western blot analysis as described below.

Biochemical assay for AB3 characterization

The HDAC-Glo™ I/II assay kit (G6420) was provided by Promega Corporation. Human recombinant C-ter-GST-HDAC 1 (H83-30G) and C-ter-HIS-HDAC 8 (H90-30H) were purchased from SignalChem. Human recombinant C-ter-HIS-HDAC 2 (50002) and N-ter-GST-HDAC 6 (50006) were purchased from BPS Bioscience and human recombinant HDAC 3/NCOR1 complex (BML-SE515) and C-ter-HIS-HDAC 10 (BML-SE559) were purchased from Enzo Life Sciences. The HDAC-Glo™ I/II assay was used as previously described (26) to determine IC_{50} values. Briefly, a 15-point 3-fold serial dilution of compound AB3 was performed at a 100× concentration in 100% DMSO in a master 96-well plate. A 5 μL aliquot of this master 100×/100% DMSO titration series was added to 245 μL of HDAC-Glo™ I/II assay buffer to generate a 2× concentrated, 2% DMSO master intermediate titration series of compound AB3 in a 96-well plate. From this master intermediate titration series, 5 μL replicates (n = 4) were transferred to a white, low-volume, round-bottom, non-binding surface 384-well assay plate (Corning 3673). An equal volume (5 μL) addition of the appropriate 2× concentrated human recombinant HDAC enzyme was then added in HDAC-Glo™ I/II assay buffer. The 10 μL human recombinant HDAC enzyme/compound AB3 inhibitor mixes were allowed to pre-incubate for 20–30 minutes at room temperature. Following this pre-incubation, an equal volume (10 μL) addition of HDAC-Glo™ I/II final detection reagent was added for a 20 μL final assay volume per well. After a 20 minute incubation at room temperature to allow the reactions to reach steady-state, luminescence was measured on a BMG CLARIOstar (BMG LABTECH).

Doxycycline inducible expression system

The plasmid containing Notch3 ICD in pcDNA 3.3 TOPO TA (Life Technologies) was obtained from Dr. Catia Giovannini (Center for Applied Biomedical Research and Departments of Internal Medicine Gastroenterology, University of Bologna, Italy). The Notch3 ICD 2.042 kb fragment was subcloned into the pRevTRE vector (Clontech) at the ClaI/BamHI sites. To create inducible TT-TRE NICD3 and TT-TRE cell lines, TT cells were transfected with regulatory plasmid pReVTet-On (Clontech) and selected in medium containing 75 μg/ml G418 (HyClone). The resulting G418 resistant, TT-Tet-on clones were transfected via Lipofectamine 2000 (Invitrogen) either with pRevTRE-Notch3 or pRevTRE plasmid to create TT-TRE NICD3 and TT-TRE cell lines, respectively. Transfected cells were selected in 50 μg/ml hygromycin (Invitrogen). Resistant TT-TRE NICD3 and TT-TRE clones were treated with doxycycline and screened for the presence of Notch3 protein by Western analysis.

Cell proliferation assay

Cells were plated in quadruplicate on 24-well plates at a density consistent with exponential growth and incubated overnight. The following day TT-TRE and TT-TRE NICD3 cells were treated with doxycycline (0, 0.2, 0.5, and 1 μg/ml)) and incubated for up to 6 days with subsequent treatments on days 2 and 4. TT and MZ-CRC-1 cells were treated with AB3 (0, 0.25, 0.5, 1, 1.5 and 2 μM) and were incubated for up to 8 days with subsequent treatments on day 2, 4 and 6. Viable cell numbers were determined by a 3-(4,5-Dimethylthiazole-2-yl)-2,5-diphenyl tetrazolium bromide (MTT) assay (Sigma) after 2, 4, and 6 days of

treatment. The assay was performed by aspirating the treatment media and adding 250 μL of serum-free media containing 0.5 mg/mL MTT (Sigma) to each well and incubating at 37°C for 4 hours. After 4 hours, 750 μL DMSO (Fisher Scientific) was added to each well and mixed. The wells were analyzed at 540 nm using a spectrophotometer (μQuant; Bio-Tek Instruments).

Flow cytometry analyses

TT-TRE and TT-TRE NICD3 cells, after 96-hour doxycycline treatment (0, 0.2, 0.5, or 1 μg/ml), and TT and MZ-CRC-1 cells, after 48-hour AB3 treatment (0, 0.25, 0.5, 1, 1.5 or 2 μM) (1×10^6), were harvested by trypsinization, and processed as previously described (25), followed by DNA content analysis using a FACScalibur (BD Biosciences) and data collection using ModFit (Verity SoftwareHouse). For sub-G_1 population analysis, the floating cells were recovered from the supernatant. To quantify apoptosis, cells (2×10^5) were treated with media or 0.2, 0.5, or 1 μg/ml doxycycline for 96 hours and harvested using non-enzymatic cell dissociation solution, Cellstripper (Cellgro). Both floating and adherent cells were collected, stained with PE Annexin V and 7 AAD fluorescein solutions (BD Pharmingen) for 15 minutes at room temperature in the dark, and flow cytometry was performed as described previously (27). Data was analyzed using FlowJo V5.0 (Tree Star, Inc.).

Western blot analysis

Cell lysates—Protein lysates were harvested from cells according to previously described protocol (28). Denatured cellular extracts were resolved by SDS-PAGE (Invitrogen), transferred onto nitrocellulose membranes (Bio-Rad Laboratories), blocked in milk (1×PBS, 5% dry skim milk, 0.05% Tween-20) or bovine serum albumin (1×PBS, 0.05% BSA (Sigma)) for 1 hour, and primary antibodies were applied for overnight incubation. The primary and secondary antibodies and their dilutions are provided in the supplementary tables S1 and S2. Following secondary antibody incubation, proteins were visualized as previously described (18,25,27).

Tumor Extracts—Tumor tissue (2 mm^3) was pulverized in the Cryoprep tissue homogenizer (Covaris) and the tissue powder was used for protein lysates preparation as described previously (29). Briefly, the tissue powder was dissolved in 500 μl of lysis buffer containing 50 mmol/l Tris, pH 7.5, 150 mmol/l NaCl, 1% Igepal CA-630, 0.1% sodium dodecyl sulfate, 0.1 μmol/l phenylmethylsulfonyl fluoride, 5 mmol/l ethylene diaminetetraacetic acid, 12 μl/ml Protease Inhibitor Cocktail (Sigma); incubated on ice for 45 minutes; and centrifuged at 13,000 RPM for 30 minutes at 4°C. The supernatants were collected, and protein concentration was determined by the bicinchoninic acid protein assay kit (Pierce). Western blot analysis for Notch3, ASCL1, and CgA expression was performed as described above.

Quantitative Real-Time PCR (qRT-PCR)

The mRNA expression levels of the extracellular region of Notch3 and Notch3 target genes *HES1, HES2, HES5 , HES6, HEY1, HEY2* were measured by qRT- PCR. RNA was isolated and transcribed into cDNA as published before (25). qRT- PCR reaction was performed

using CFX Thermal Cycler and SsoFast EvaGreen labeling system (Bio-Rad) at conditions described earlier (18) on three biological replicates. The primer sequences are provided in the supplementary table S3. The cycle numbers obtained at the log-linear phase of the reactions for target genes were normalized to housekeeping gene *s27* from the same sample measured concurrently. Finally, the expression ratios were calculated using the comparative cycle threshold (ΔCt) method and presented as average ± standard error of the mean (SEM).

Luciferase reporter assay

Notch3 functional activity was measured, by the degree of CBF1-binding, utilizing a luciferase construct containing four CBF1-binding sites (4×CBF1-Luc). TT-TRE and TT-TRE NICD3 cell lines or TT and MZ-CRC-1 cell lines were transiently transfected with CBF1-luciferase reporter construct and then treated with 0–1 μg/ml doses of doxycycline or 0–2μM doses of AB3 for 48 hours. To normalize for transfection efficiency, 0.5 μg of cytomegalovirus β-galactosidase (CMV-β-gal) was cotransfected as described in details (13).

Notch3 RNA interference assay

Small interfering RNA (siRNA) against Notch3 or nonspecific siRNA (Santa Cruz Biotechnology) were transfected into TT cells using Lipofectamine RNAiMAX (Invitrogen) according to manufacturer's instruction. After 24h incubation, cells were treated with DMSO or AB3 (1.5μM) for additional 48 hours followed by mRNA isolation for qRT-PCR analyses. For the MTT cell proliferation analyses (as described above) TT cells were incubated for 24, 48 and 72h after AB3 treatment and viable cells were calculated at each timpoint. Additionally, to confirm that increased proliferation is due to Notch3 silencing, qRT-PCR was performed to detect Notch3 expression at each time point.

Animal studies

Four-week-old male athymic nude mice were obtained from Charles Rivers Laboratories. They were allowed to acclimate one week in the animal facility to reduce stress after arrival. Mice were maintained under specific pathogen-free conditions. TT-TRE NICD3 and TT-TRE cell lines xenograft tumors were established by implanting 10^7 cells in 200 μl of Hanks Balanced Salt Solution (Mediatech) subcutaneously into the left flank of five weeks old mice. Two weeks after inoculation, mice with palpable tumors were randomized into two control groups (TT-TRE NICD3; n=5 and TT- TRE; n=6) receiving a standard diet of irradiated feed and two treated groups (TT-TRE NICD3; n=5 and TT- TRE; n=6) receiving a doxycycline diet of irradiated feed containing 625 mg of doxycycline per 1 kg of feed (Harlan-Teklad) (30). Treatments continued for 36 days. Tumor volumes were measured by external caliper every four days and then were calculated by the modified ellipsoidal formula: Tumor volume = ½ (length×width^2). At the end of the experiment, mice were sacrificed and the tumors were dissected from the surrounding tissues and flash frozen in liquid nitrogen for storage in −80°C. Postmortem examination of the lungs, liver, kidneys, and spleen were performed to confirm that there was no evidence of metastases or tumor growth outside of the inoculation site. All experimental procedures were done in compliance with our animal care protocol approved by the University of Wisconsin-Madison Animal Care and Use Committee.

Statistics

Data are expressed as mean ± SE. Statistical analyses were done by two-way ANOVA followed by a protected Fisher's LSD for post hoc comparisons or by the Student *t* test to compare two groups. All analyses were conducted using SAS 9.3 (SAS Institute, Cary NC) software. A p-value < 0.05 was considered statistically significant in two-tailed statistical tests.

Results

Notch3 signaling in MTC cells

We examined Notch3 expression in human cancer cells lines and tumor samples. Using Western blot analysis we demonstrated that human MTC TT and MZ-CRC-1 cell lines lacked the full length and intracellular domain of Notch3 (NICD3) while nontumorigenic human thyroid epithelial cell lines HTori-3 and Nthy-ori 3-1 and pancreatic cancer MIA-PaCa-2 and ovarian cancer OVCAR-3 cell lines had high Notch3 levels (Fig. 1A). Similarly, human MTC tumors from patients with sporadic and inherited MTC also lacked both portions of Notch3 while human ovarian and colorectal cancer specimens had detectable levels of full length and cleaved Notch3 (Fig. 1B). These results suggest that lack of NICD3 in MTC cell lines and MTC cancer specimens is due to impaired expression of full length Notch3. The NE origin of the MTC cell lines and tumor samples were verified by high levels of ASCL1 and CgA.

In order to determine the effect of restoration of Notch3 in human MTC cells, we stably transfected MTC TT cells with a doxycycline-inducible NICD3 (active Notch3) construct creating TT-TRE NICD3 cells. As shown in figure 1C, in the absence of doxycycline, there is no NICD3 protein. However, increasing doses of doxycycline in TT-TRE NICD3 led to a dose-dependent corresponding increase in NICD3 protein. Transfection with the empty vector construct (TT-TRE) lacked NICD3 at baseline and also with doxycycline treatment. To show that the expressed NICD3 protein was functional, TT-TRE and TT-TRE NICD3 cells were transiently transfected with a CBF-1 luciferase reporter construct. CBF-1 binding is critical for Notch signaling. As shown in figure 1D, while doxycycline treatment in TT-TRE cells slightly reduced luciferase activity, doxycycline-mediated induction of NICD3 in TT-TRE NICD3 cells resulted in a marked dose-dependent increase in luciferase activity indicating increasing CBF-1 binding and functional NICD3.

We then confirmed if the other components of Notch3 signaling were intact in human MTC cells. As previously mentioned, functional downstream targets of Notch3 include HES and HEY proteins. NICD3 has been shown to upregulate HES1, HES5, HEY1, and HEY2 while inhibiting HES2 and HES6 (31,32). As predicted, doxycycline induction of NICD3 in TT-TRE NICD3 cells resulted in increases in HES1, HES5, HEY1, and HEY2 mRNA and decreases in HES2 and HES6 (Fig. 1E). These changes were not observed in the TT-TRE cells. Thus, these data demonstrate that while Notch3 is absent in human MTCs, restoration of functional Notch3 protein (NICD3) leads to induction of the Notch3 signaling pathway.

Notch3 expression in MTC cells alters the NE phenotype and cellular proliferation

Notch3 is known to downregulate ASCL1, which is overexpressed in a variety of NE cancers (33) . Treatment of TT-TRE NICD3 cells with doxycycline resulted in a dose-dependent decrease in ASCL1 protein (Fig. 2A). We also examined the effect of Notch3 on other NE tumor markers such as CgA, calcitonin, and SYP. As shown in figure 2A, overexpression of NICD3 led to marked reductions in these NE markers as well. To determine if the downregulation of these NE peptides/hormones was dependent on the continuing presence of NICD3, we performed withdrawal experiments. After 2 days of doxycycline treatment in TT-TRE NICD3 cells, the cells were placed in doxycycline-free media. As shown in figure 2B, 2 days after doxycycline withdrawal, the NICD3 disappeared. The absence of NICD3 eventually resulted in a return of ASCL1 and CgA to baseline levels after 6 additional days. Therefore, the NE phenotype of MTC is tightly controlled by Notch3.

To determine the effect of Notch3 on MTC cellular proliferation, MTT assays were performed on TT-TRE NICD3 (Fig. 2C) and TT-TRE (Fig. 2D) cells with varying dosages of doxycycline. Increasing levels of NICD3, produced by doxycycline treatment of TT-TRE NICD3 cells, results in dose-dependent inhibition of MTC cellular proliferation (Fig. 2C and 2E). In fact, the highest levels of doxycycline induced NICD3 expression led to complete cessation of tumor cell growth. Doxycycline had no effect on TT-TRE cell proliferation (Fig. 2D).

To delineate the mechanism of Notch3-mediated MTC growth inhibition we performed the flow cytometry experiments. As shown in figures 3A and 3B, conditional induction of NICD3 in TT-TRE NICD3 cells resulted in dose-dependent accumulation of sub-G_1 DNA which was not observed in TT-TRE control cells. The percentage of preapoptoic versus apopotoic MTC cells was quanitified using PE AnnexinV/7AAD staining (Fig. 3C and 3D). High levels of apopotosis were observed with NICD3 induction in MTC cells. Additionally, apoptosis was verified by Western blot as shown in Fig. 3E. Induction of NICD3 by doxycycline treatment in TT-TRE NICD3 cells led to increases in cleaved PARP and p27 with corresponding reductions in Mcl-1, p21, and cyclin D1.

Notch3 can self-regulate

We have shown that Notch3 tightly regulates MTC phenotype and proliferation. In this system, high levels of active Notch3 (NICD3) can be generated. We then investigated whether the rapid increase in NICD3 levels could also be due to auto-induction of endogenous Notch3 protein. We therefore measured Notch3 mRNA levels after NICD3 induction in TT-TRE NICD3 cells using primers in the Notch3 extracellular region (outside NICD3, described in supplementary Fig. S1A). As shown in supplementary Fig. S1B, mRNA levels of the Notch3 extracellular domain were similar in TT-TRE cells treated with doxycycline and vehicle, and in TT-TRE NICD3 cells treated with vehicle. However, TT-TRE NICD3 cells treated with doxycycline had high levels of Notch3 mRNA extracellular region. This induction of endogenous Notch3 mRNA results in high levels of the Notch3 full-length receptor protein (supplementary Fig. S1C). Thus, Notch3 appears to have the capacity to autoregulate its own expression.

Notch3 inhibits MTC growth *in vivo*

Utlizing a MTC xenograft model, we studied the effect of NICD3 induction *in vivo*. MTC xenografts were established in nude mice using TT-TRE and TT-TRE NICD3 cells. MTC tumors from TT-TRE cells treated with vehicle and doxycycline had robust proliferation (Fig. 4A). Similarly, tumors from TT-TRE NICD3 cells treated with vehicle also continued to grow in this model. However, in sharp contrast, NICD3 induction in TT-TRE NICD3 cells with doxycycline treatment markedly inhibited MTC tumor proliferation (Fig. 4A). As expected and similar to the *in vitro* conditions, induction of NICD3 in MTC tumors resulted in downregulation of the NE marker ASCL1 and an increase in apoptosis as measured by cleaved PARP (Fig. 4B).

Identification of a small molecule which induces Notch3 and alters neuroendocrine phenotype in MTC

Having demonstrated that induction of Notch3 in MTC cells inhibits cancer cell proliferation both *in vitro* and *in vivo*, we were interested in the concept of activating Notch3 as a therapeutic target. Furthermore, since Notch3 also suppresses NE peptide/hormone levels, this strategy could be used to palliate patients with endocrinopathies which are commonly associated with this disease. Thus, we sought to identify a small molecule which induces Notch3 in MTC cells. We had previously developed a high throughput screen for Notch activating compounds (34). Utilizing this system, we identified a synthetic compound, AB3, which appeared to have this property. AB3 is a histone deacetylase inhibitor (Fig. 5A). It was prepared by condensing commercially available para-methoxybenzaldehyde with a known bifunctional reagent, which has a six methylene carbon tether between a hydrazide and a hydroxamic acid (24). As shown in figure 5B, exposure of TT cells to AB3 led to a dose-dependent induction in Notch3 mRNA. This induction was specific to Notch3, as AB3 did not affect mRNA levels of Notch1 or Notch2. To determine if AB3 induces both full-length of Notch3 and NICD3 in MZ-CRC-1 and TT cell lines, qRT-PCR was used with primers that recognize the extracellular region of Notch3 - NECD3 (supplementary Fig. S2A and S2B) or primers specific for the intracellular domain –NICD3 (Supplementary Fig.S2C and S2D). We revealed that AB3 induces both the full length Notch3 and NICD3 to significantly higher levels than control treated cells. This increase in Notch3 led to an induction of functional NICD3 in both MTC TT and MZ-CRC-1 cells as demonstrated by elevated CBF-1 binding activity (Fig. 5C and 5D). To further validate if AB3 acts as a functional Notch3 activating compound in MTC cell lines we performed Western blot analysis to detect the intracellular domain of Notch3 protein (Fig. 5E and 5F).

Similar to NICD3 induction in our doxycycline-inducible model, treatment of MTC cells by AB3 also led to downregulation of NE tumor markers ASCL1 and CgA (Fig. 5G and 5H). We then investigated the effects of AB3 on MTC cellular proliferation. AB3 suppressed growth in both MTC TT (Fig. 6A) and MZ-CRC-1 (Fig. 6B) cell lines in a dose-dependent manner. As with genetic induction of NICD3, AB3 treatment also caused apoptosis in TT and MZ-CRC-1 cells as demonstrated by cleaved PARP, reduction of XIAP, survivin, p21 and overexpression of p27 through Western analysis (Fig. 6C), as well as by sub-G_1 DNA accumulation with flow cytometry experiments (Fig. 6D, 6E, and 6F).

Biochemical characterization of HDAC inhibitor, AB3

In order to assess the inhibitory activity and selectivity of AB3 to specific HDAC isoenzymes, we used the HDAC-Glo™ I/II luminescent assay which measures the relative activity of HDAC class I and IIb enzymes from purified enzymes, cells, or cell extracts. Using this assay, first we determined the optimal concentration of purified human recombinant HDAC's to use per reaction. The optimal concentrations of the listed HDAC isoenzymes (Fig.7A) were in the lower end of the linear portion of the enzyme titration assay and concentrations were also chosen so all HDAC isoforms gave similar luminescent signal (RLU) output (enzyme titration not shown). Next, we determined the IC50 of AB3 against the indicated purified human recombinant HDAC isoforms and showed that AB3 appears to be HDAC 1, 2, and 3 selective with less inhibitory potency against the HDAC 6, 8, and 10 isoforms (Fig.7A and Table. 1). Furthermore, utilizing the HDAC-Glo™ I/II luminescent assay, we demonstrated the inhibition of HDAC activity in the MZ-CRC-1 and TT cell lines using AB3 as the HDAC inhibitor. This experiment revealed that AB3 reaches its maximal inhibitory activity in a range of 1–10μM in both MTC cell lines (Fig.7B and 7C). Interestingly, the dose of 2 μM of AB3 exerted the highest induction of Notch3 expression in MZ-CRC-1 and TT cell lines.

Notch3 interference blocks the phenotypic effects of AB3 in MTC cells

To confirm that the phenotypic effect of AB3 (i.e. inhibition of ASCL1 and CgA protein expression and reduction of MTC cell proliferation) are a result of activation of Notch3 signaling, siRNA targeting Notch3 were used to silence the gene expression. MTC TT cells were transiently transfected with Notch3 or nonspecific siRNA and 24 hours later treated with vehicle or AB3. Using qRT-PCR analysis we demonstrated that Notch3 targeted siRNA were capable to significantly reduce AB3-activated Notch3 (Fig.8A) and downstream HES1 message levels (Fig.8B) following AB3 treatment. Moreover, blockade of AB3-mediated Notch 3 activation reversed the AB3 induced changes in ASCL1 and CgA expression (Fig.8C). Finally, the abrogation of AB3-mediated Notch3 induction by Notch3 siRNA resulted in increased proliferation of TT cells (Fig.8D). These data suggest that phenotypic regulation with AB3 treatment was primarily mediated by Notch3 signalling.

Discussion

Although intracellular Notch signal transduction seems to be very simple, in human cancer cells the Notch pathway exerts pleiotropic functions. So far, Notch1 is the best characterized isoform with dual action potency which, depending upon the cellular context, may act as a tumor suppressor or as an oncogene. The first evidence for the oncogenic role of Notch1 came from human T-cell neoplasia (35). Later, it was shown that Notch1 was up-regulated in various solid tumors, including breast cancer (36), medulloblastoma (37), colorectal cancer (38), and non-small cell lung carcinoma (NSCLC) (39). The contribution of Notch1 to tumorigenesis in these cancers is mainly through maintaining cells in the proliferation stage by inhibiting apoptosis. Conversely, Notch1 signaling is very minimal or absent in NE cancers such as small cell lung cancer (SCLC), pancreatic carcinoid, and MTC, where reinstitution of Notch1 by either pharmacological or genetic approach inhibits the tumorigenic process (13,40,41). Additionally, in the skin, Notch1 loss of function results in

spontaneous basal cell carcinomas (42). These apparent but paradoxical functions clearly indicate that the role of Notch1 signaling is dependent on its cellular context.

While the dual role of Notch1 in human cancers has been extensively studied, there are far less data regarding Notch3. Studies to date have mainly described the role of Notch as an oncogene. Notch3 signaling has been implicated as an oncogene in ovarian serous carcinomas where amplification of the *Notch3* genomic locus is critical for cellular survival and growth . Additionally, translocation of the *Notch3* gene occurs in a subset of non-small-cell lung cancer (43), and constitutively expressed Notch3 induces neoplastic transformation in the breast, brain, colon, and hematopoietic tissues (44–48). Moreover, using an RNAi approach, Notch3, but not Notch1, was found to be critical in maintaining cellular proliferation of ErbB2-negative breast cancers (46).

In contrast, there are little data regarding the tumor suppressor role of Notch3 in human malignancies. Demehri et al. (42) showed that mice lacking Notch3 in the skin developed skin-barrier defects, epidermal hyperplasia, and skin tumors. More recently, it has been shown that up-regulation of Notch3 is sufficient to activate senescence and inhibit proliferation in breast, melanoma, and glioblastoma cell lines (49). Thus, similar to Notch1, Notch3 may also have a dual role in cancer as an oncogene or tumor suppressor depending on the cellular context. To date, the role of Notch3 in endocrine malignancies, such as thyroid cancer and NE cancers, has not been explored.

In this paper, we demonstrate for the first time that Notch3 acts as a tumor suppressor in human MTC. Notch3 protein is not expressed in human MTC tumor samples and cell lines but detectable in nontumorigenic human thyroid epithelial cell lines. To restore normal thyroid phenotype for Notch3 expression and elucidate its role we created a gain-of-function model by generating MTC cells with a doxycycline-inducible Notch3 intracellular domain (NICD3). We show that forced NICD3 expression in MTC does not promote but indeed inhibits tumor cell proliferation by triggering apoptotic events in a dose-dependent fashion. Importantly, NICD3 induction leads to the functional activation of the Notch3 mediator CBF1, followed by changes in transcriptional levels of HES and HEY genes. Moreover, Notch3 activation causes a reduction of NET markers ASCL1, CgA, calcitonin, and SYP, indicating that this pathway is conserved in MTC. We also verify that Notch3 activity is required *in vivo* to reduce the growth rate of MTC xenografts.

MTC is derived from the NE C-cells of the thyroid and is one of the more aggressive subtypes of thyroid cancer. Like most thyroid cancers, surgical resection is the predominant treatment modality and can be curative in selected patients. However, unlike well-differentiated thyroid cancer which can be treated with surgery and/or radioactive iodine even when metastases develop, patients with MTC have limited options. For decades, there were no approved drugs to treat patients with metastatic MTC. Recently, the FDA has approved two compounds for metastatic MTC (9). Although both of these drugs were shown in clinical trials to prolong recurrence-free survival, their effect on long-term survival is unknown.

Currently, the approved therapies for MTC have targeted the inhibition of RET signaling. This concept is based on the important fact that mutations in the RET proto-oncogene have been shown to cause inherited MTC in multiple endocrine neoplasia (MEN) type 2A, MEN2B, and familial MTC (9,10). In fact, genetic testing for *RET* mutations in children from families with inherited MTC, and age-appropriate prophylactic removal of the thyroid gland, has been shown to be curative in these patients (50). However, in patients with inherited MTC diagnosed later in life after the MTC has metastasized, surgery is not curative, and RET inhibitors are the mainstay of therapy. In addition, the majority of patients with sporadic MTC also have somatic, activating mutations in *RET* (9,10,50). Therefore, patients with metastatic inherited and sporadic MTC are currently treated with targeted therapies against RET. However, although tyrosine kinase inhibitors which block RET function are very effective in the lab, they do not appear to have any effect on overall patient survival in several clinical trials. Therefore, there is a clear need for alternative options which target other pathways important for MTC progression. While most research in MTC has focused on RET, emerging data suggest that other pathways, such as CDK5 and Notch, may play essential role in MTC development and progression (13,18,40,51).

In this paper, we identify a small molecule which can induce Notch3 signaling in MTC cells. To our knowledge, this is the first description of a compound which specifically activates Notch3 signaling. We demonstrate that AB3 induces Notch3 signaling, inhibits MTC proliferation, and suppresses NE tumor markers. These effects are achieved at low micromolar drug doses. AB3 would be an candidate for *in vivo* models and preliminary clinical studies identifying safe and appropriate dosing parameters and pharmacokinetics as an initial phase to further clinical investigation. It is possible that AB3 could be used in conjuction with tyrosine kinase inhibitors, and this combination is currently under investigation in our lab.

In summary, this study documents the tumor suppressing role of Notch3 in MTC in both *in vitro* and *in vivo* models, providing the rationale for targeting Notch3 with small molecule compounds to treat patients with MTC and other tumors in which this pathway is not active.

Supplementary Material

Refer to Web version on PubMed Central for supplementary material.

Acknowledgments

The authors thank Dr. Muthusamy Kunnimalaiyaan for his critical suggestions during the study, Yash Somnay for the composition and Heather Hardin for the valuable suggestions for culturing nontumorigenic thyroid epithelial cell lines.

Grant support

This work was supported by grants NIH (R01 CA121115, to H. Chen), American Cancer Society (MEN2 Thyroid Cancer Professorship 120319-RPM-11-080-01-TBG to H. Chen and Research Scholar Award RSGM TBE-121413 to H.Chen), and Layton F. Rikkers, MD, Chair in Surgical Leadership Professorship (H. Chen).

References

1. Udelsman R, Chen H. The current management of thyroid cancer. Adv Surg. 1999; 33:1–27. [PubMed: 10572560]
2. Chen H, Kunnimalaiyaan M, Van Gompel JJ. Medullary thyroid cancer: the functions of raf-1 and human achaete-scute homologue-1. Thyroid. 2005; 15(6):511–521. [PubMed: 16029117]
3. Greenblatt DY, Elson D, Mack E, Chen H. Initial lymph node dissection increases cure rates in patients with medullary thyroid cancer. Asian J Surg. 2007; 30(2):108–112. [PubMed: 17475579]
4. Hahm JR, Lee MS, Min YK, Lee MK, Kim KW, Nam SJ, et al. Routine measurement of serum calcitonin is useful for early detection of medullary thyroid carcinoma in patients with nodular thyroid diseases. Thyroid. 2001; 11(1):73–80. [PubMed: 11272100]
5. Chen H, Roberts JR, Ball DW, Eisele DW, Baylin SB, Udelsman R, et al. Effective long-term palliation of symptomatic, incurable metastatic medullary thyroid cancer by operative resection. Ann Surg. 1998; 227(6):887–895. [PubMed: 9637552]
6. Kebebew E, Kikuchi S, Duh QY, Clark OH. Long-term results of reoperation and localizing studies in patients with persistent or recurrent medullary thyroid cancer. Arch Surg. 2000; 135(8):895–901. [PubMed: 10922248]
7. Roman S, Lin R, Sosa JA. Prognosis of medullary thyroid carcinoma: demographic, clinical, and pathologic predictors of survival in 1252 cases. Cancer. 2006; 107(9):2134–2142. [PubMed: 17019736]
8. Wells SA, Gosnell JE, Gagel RF, Moley J, Pfister D, Sosa JA, et al. Vandetanib for the treatment of patients with locally advanced or metastatic hereditary medullary thyroid cancer. J Clin Oncol. 2010; 28(5):767–772. [PubMed: 20065189]
9. Roy M, Chen H, Sippel RS. Current understanding and management of medullary thyroid cancer. Oncologist. 2013; 18(10):1093–1100. [PubMed: 24037980]
10. Chen H, Sippel RS, O'Dorisio MS, Vinik AI, Lloyd RV, Pacak K. The North American Neuroendocrine Tumor Society consensus guideline for the diagnosis and management of neuroendocrine tumors: pheochromocytoma, paraganglioma, and medullary thyroid cancer. Pancreas. 2010; 39(6):775–783. [PubMed: 20664475]
11. Chen H, Biel MA, Borges MW, Thiagalingam A, Nelkin BD, Baylin SB, et al. Tissue-specific expression of human achaete-scute homologue-1 in neuroendocrine tumors: transcriptional regulation by dual inhibitory regions. Cell Growth Differ. 1997; 8(6):677–686. [PubMed: 9186001]
12. Sippel RS, Carpenter JE, Kunnimalaiyaan M, Chen H. The role of human achaete-scute homolog-1 in medullary thyroid cancer cells. Surgery. 2003; 134(6):866–871. discussion 71–3. [PubMed: 14668716]
13. Kunnimalaiyaan M, Vaccaro AM, Ndiaye MA, Chen H. Overexpression of the NOTCH1 intracellular domain inhibits cell proliferation and alters the neuroendocrine phenotype of medullary thyroid cancer cells. J Biol Chem. 2006; 281(52):39819–39830. [PubMed: 17090547]
14. Kameda Y, Nishimaki T, Miura M, Jiang SX, Guillemot F. Mash1 regulates the development of C cells in mouse thyroid glands. Dev Dyn. 2007; 236(1):262–270. [PubMed: 17103415]
15. Ball DW. Achaete-scute homolog-1 and Notch in lung neuroendocrine development and cancer. Cancer Lett. 2004; 204(2):159–169. [PubMed: 15013215]
16. Fortini ME. Notch signaling: the core pathway and its posttranslational regulation. Dev Cell. 2009; 16(5):633–647. [PubMed: 19460341]
17. Sriuranpong V, Borges MW, Strock CL, Nakakura EK, Watkins DN, Blaumueller CM, et al. Notch signaling induces rapid degradation of achaete-scute homolog 1. Mol Cell Biol. 2002; 22(9):3129–3139. [PubMed: 11940670]
18. Jaskula-Sztul R, Pisarnturakit P, Landowski M, Chen H, Kunnimalaiyaan M. Expression of the active Notch1 decreases MTC tumor growth in vivo. J Surg Res. 2011; 171(1):23–27. [PubMed: 21571316]
19. Maillard I, Pear WS. Notch and cancer: best to avoid the ups and downs. Cancer Cell. 2003; 3(3): 203–205. [PubMed: 12676578]

20. Yoon K, Gaiano N. Notch signaling in the mammalian central nervous system: insights from mouse mutants. Nat Neurosci. 2005; 8(6):709–715. [PubMed: 15917835]
21. Kopan R. Notch signaling. Cold Spring Harb Perspect Biol. 2012; 4(10)
22. Fryer CJ, White JB, Jones KA. Mastermind recruits CycC:CDK8 to phosphorylate the Notch ICD and coordinate activation with turnover. Mol Cell. 2004; 16(4):509–520. [PubMed: 15546612]
23. Kopan R, Ilagan MX. The canonical Notch signaling pathway: unfolding the activation mechanism. Cell. 2009; 137(2):216–233. [PubMed: 19379690]
24. Tang W, Luo T, Greenberg EF, Bradner JE, Schreiber SL. Discovery of histone deacetylase 8 selective inhibitors. Bioorg Med Chem Lett. 2011; 21(9):2601–2605. [PubMed: 21334896]
25. Tesfazghi S, Eide J, Dammalapati A, Korlesky C, Wyche TP, Bugni TS, et al. Thiocoraline alters neuroendocrine phenotype and activates the Notch pathway in MTC-TT cell line. Cancer Medicine. 2013; 2(5):734–743. [PubMed: 24403239]
26. Halley F, Reinshagen J, Ellinger B, Wolf M, Niles AL, Evans NJ, et al. A bioluminogenic HDAC activity assay: validation and screening. J Biomol Screen. 2011; 16(10):1227–1235. [PubMed: 21832257]
27. Yu XM, Jaskula-Sztul R, Ahmed K, Harrison AD, Kunnimalaiyaan M, Chen H. Resveratrol induces differentiation markers expression in anaplastic thyroid carcinoma via activation of Notch1 signaling and suppresses cell growth. Mol Cancer Ther. 2013; 12(7):1276–1287. [PubMed: 23594881]
28. Sippel RS, Carpenter JE, Kunnimalaiyaan M, Lagerholm S, Chen H. Raf-1 activation suppresses neuroendocrine marker and hormone levels in human gastrointestinal carcinoid cells. Am J Physiol Gastrointest Liver Physiol. 2003; 285(2):G245–G254. [PubMed: 12851216]
29. Vaccaro A, Chen H, Kunnimalaiyaan M. In-vivo activation of Raf-1 inhibits tumor growth and development in a xenograft model of human medullary thyroid cancer. Anticancer Drugs. 2006; 17(7):849–853. [PubMed: 16926634]
30. Cawthorne C, Swindell R, Stratford IJ, Dive C, Welman A. Comparison of doxycycline delivery methods for Tet-inducible gene expression in a subcutaneous xenograft model. J Biomol Tech. 2007; 18(2):120–123. [PubMed: 17496224]
31. Wang W, Campos AH, Prince CZ, Mou Y, Pollman MJ. Coordinate Notch3-hairy-related transcription factor pathway regulation in response to arterial injury. Mediator role of platelet-derived growth factor and ERK. J Biol Chem. 2002; 277(26):23165–23171. [PubMed: 11971902]
32. Shimizu K, Chiba S, Saito T, Kumano K, Hamada Y, Hirai H. Functional diversity among Notch1, Notch2, and Notch3 receptors. Biochem Biophys Res Commun. 2002; 291(4):775–779. [PubMed: 11866432]
33. Cook M, Yu XM, Chen H. Notch in the development of thyroid C-cells and the treatment of medullary thyroid cancer. Am J Transl Res. 2010; 2(1):119–125. [PubMed: 20182588]
34. Pinchot SN, Jaskula-Sztul R, Ning L, Peters NR, Cook MR, Kunnimalaiyaan M, et al. Identification and validation of Notch pathway activating compounds through a novel high-throughput screening method. Cancer. 2011; 117(7):1386–1398. [PubMed: 21425138]
35. Ellisen LW, Bird J, West DC, Soreng AL, Reynolds TC, Smith SD, et al. TAN-1, the human homolog of the Drosophila notch gene, is broken by chromosomal translocations in T lymphoblastic neoplasms. Cell. 1991; 66(4):649–661. [PubMed: 1831692]
36. Hao L, Rizzo P, Osipo C, Pannuti A, Wyatt D, Cheung LW, et al. Notch-1 activates estrogen receptor-alpha-dependent transcription via IKKalpha in breast cancer cells. Oncogene. 2010; 29(2):201–213. [PubMed: 19838210]
37. Natarajan S, Li Y, Miller EE, Shih DJ, Taylor MD, Stearns TM, et al. Notch1-induced brain tumor models the sonic hedgehog subgroup of human medulloblastoma. Cancer Res. 2013; 73(17):5381–5390. [PubMed: 23852537]
38. Sikandar SS, Pate KT, Anderson S, Dizon D, Edwards RA, Waterman ML, et al. NOTCH signaling is required for formation and self-renewal of tumor-initiating cells and for repression of secretory cell differentiation in colon cancer. Cancer Res. 2010; 70(4):1469–1478. [PubMed: 20145124]

39. Ji X, Wang Z, Geamanu A, Goja A, Sarkar FH, Gupta SV. Delta-tocotrienol suppresses Notch-1 pathway by upregulating miR-34a in nonsmall cell lung cancer cells. Int J Cancer. 2012; 131(11): 2668–2677. [PubMed: 22438124]
40. Kunnimalaiyaan M, Traeger K, Chen H. Conservation of the Notch1 signaling pathway in gastrointestinal carcinoid cells. Am J Physiol Gastrointest Liver Physiol. 2005; 289(4):G636–G642. [PubMed: 16160079]
41. Sriuranpong V, Borges MW, Ravi RK, Arnold DR, Nelkin BD, Baylin SB, et al. Notch signaling induces cell cycle arrest in small cell lung cancer cells. Cancer Res. 2001; 61(7):3200–3205. [PubMed: 11306509]
42. Demehri S, Turkoz A, Kopan R. Epidermal Notch1 loss promotes skin tumorigenesis by impacting the stromal microenvironment. Cancer Cell. 2009; 16(1):55–66. [PubMed: 19573812]
43. Dang TP, Gazdar AF, Virmani AK, Sepetavec T, Hande KR, Minna JD, et al. Chromosome 19 translocation, overexpression of Notch3, and human lung cancer. J Natl Cancer Inst. 2000; 92(16): 1355–1357. [PubMed: 10944559]
44. Hu C, Dievart A, Lupien M, Calvo E, Tremblay G, Jolicoeur P. Overexpression of activated murine Notch1 and Notch3 in transgenic mice blocks mammary gland development and induces mammary tumors. Am J Pathol. 2006; 168(3):973–990. [PubMed: 16507912]
45. Yamaguchi N, Oyama T, Ito E, Satoh H, Azuma S, Hayashi M, et al. NOTCH3 signaling pathway plays crucial roles in the proliferation of ErbB2-negative human breast cancer cells. Cancer Res. 2008; 68(6):1881–1888. [PubMed: 18339869]
46. Pierfelice TJ, Schreck KC, Dang L, Asnaghi L, Gaiano N, Eberhart CG. Notch3 activation promotes invasive glioma formation in a tissue site-specific manner. Cancer Res. 2011; 71(3): 1115–1125. [PubMed: 21245095]
47. Serafin V, Persano L, Moserle L, Esposito G, Ghisi M, Curtarello M, et al. Notch3 signalling promotes tumour growth in colorectal cancer. J Pathol. 2011; 224(4):448–460. [PubMed: 21598247]
48. Bellavia D, Campese AF, Alesse E, Vacca A, Felli MP, Balestri A, et al. Constitutive activation of NF-kappaB and T-cell leukemia/lymphoma in Notch3 transgenic mice. Embo j. 2000; 19(13): 3337–3348. [PubMed: 10880446]
49. Kadesch T. Notch signaling: the demise of elegant simplicity. Curr Opin Genet Dev. 2004; 14(5): 506–512. [PubMed: 15380241]
50. Shepet K, Alhefdhi A, Lai N, Mazeh H, Sippel R, Chen H. Hereditary medullary thyroid cancer: age-appropriate thyroidectomy improves disease-free survival. Ann Surg Oncol. 2013; 20(5): 1451–1455. [PubMed: 23188542]
51. Pozo K, Castro-Rivera E, Tan C, Plattner F, Schwach G, Siegl V, et al. The role of Cdk5 in neuroendocrine thyroid cancer. Cancer Cell. 2013; 24(4):499–511. [PubMed: 24135281]

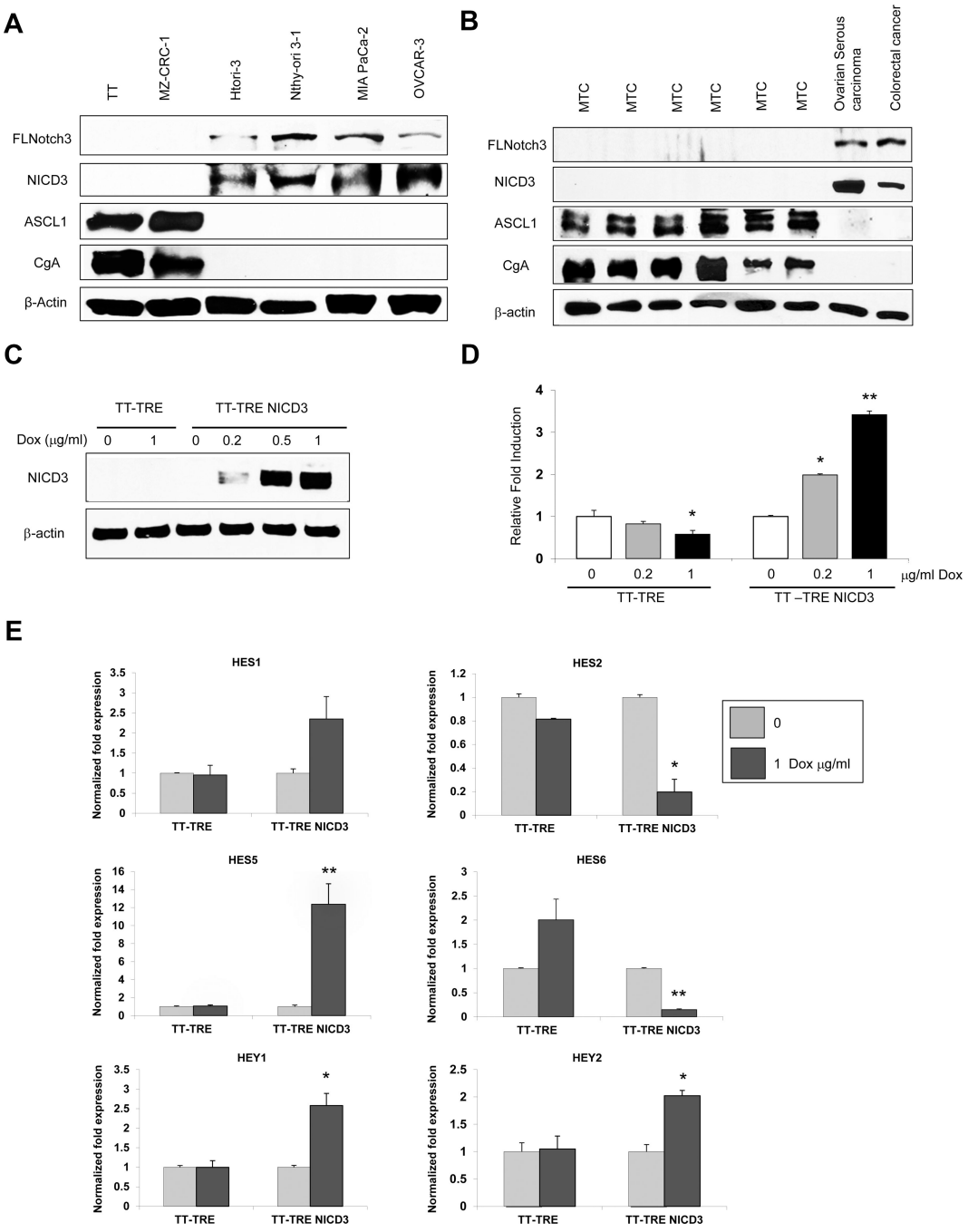

Figure 1. Induced Notch3 pathway is active in MTC-TT cells

Expression pattern of Notch3 in (**A**) various human cell lines and (**B**) tumor samples analyzed by Western blot. MTC tumors and cell lines are positive for NET markers ASCL1 and CgA but lack full length and intracellular portion of Notch3 (NICD3). (**C**) Western blot analysis of doxycycline dose-responded induction of NICD3 in TT-TRE NICD3 cells, and lack of NICD3 protein in TT-TRE control cells after 4 days of treatment. β-actin was used as a loading control. (**D**) Analysis of NICD3 function by the degree of NICD3–CBF1 binding measured by luciferase reporter assay. Treatment with increasing concentrations of

doxycycline resulted in concurrent increase in relative luciferase activity compared with the control (no doxycycline) in TT-TRE NICD3 cells. The decrease in luciferase activity in the control cell line, TT-TRE, suggests an inhibitory effect of doxycycline on luciferase. Luciferase values were normalized to β-galactosidase activity and are expressed as fold increase relative to untreated cells. All values are presented as a mean ±SD (n=3). (**E**) qRT-PCR expression analysis of Notch3 signaling mediators HES1, HES2, HES5, HES6, HEY1, and HEY2. Cycle numbers obtained at the log-linear phase were normalized to housekeeping gene s27 from the same sample measured concurrently. The expression ratios were calculated using the comparative cycle threshold (ΔCt) method. All values are presented as a mean ±SD (n=3). The effect of doxycycline on the control cell line (TT-TRE) showed no change or no significant change. *, $P<0.05$, **, $P<0.01$.

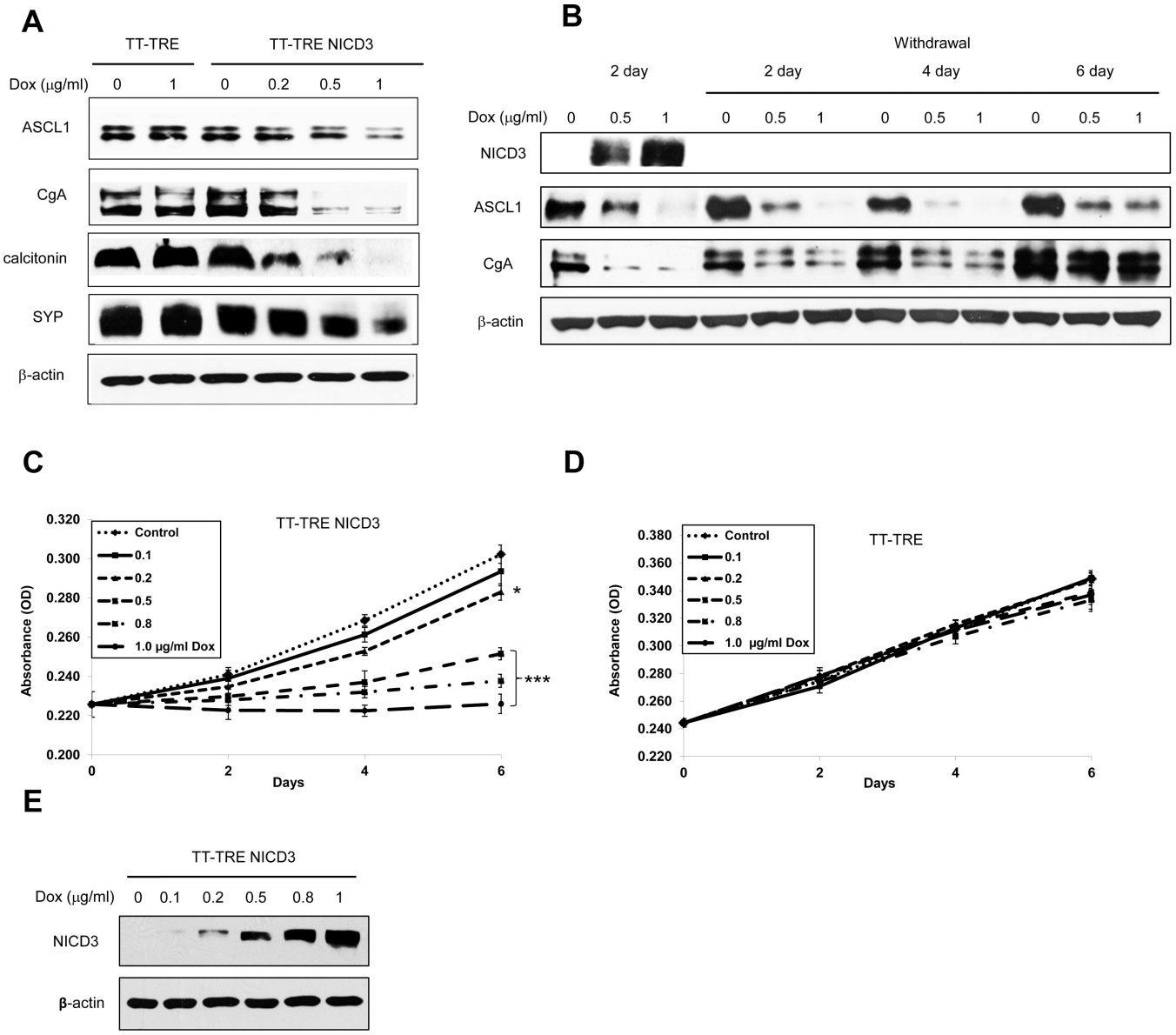

Figure 2. NICD3 activation alters neuroendocrine phenotype of MTC-TT cells

(**A**) Western blot analysis of reduction NE markers, ASCL1, CgA, calcitonin, and SYP. The same concentration of doxycycline caused no effect on NE marker expression in vector control cells (TT-TRE). Western blots represent cell lysates obtained after 4 days of doxycycline treatment. (**B**) The longer-term effect of active NICD3 on NE expression was evaluated by treating TT-TRE NICD3 cells with 0.5 and 1 μg/ml of doxycycline for 2 days, then replacing with doxycycline free media for another 6 days, with lysates isolated at each 2 day increment. NICD3 protein was present only in 2 day doxycycline-treated cells indicating that constant induction is required for NICD3 expression. The greatest reduction in NE markers ASCL1 and CgA was observed at 4 days of doxycycline withdrawal (NICD3 was not detected); indicating both delayed and prolonged effect of active NICD3 on downstream mediators. Note that at the later time points the levels of ASCL1 and CgA return to near the control cell level. Equal loading was confirmed with anti β-actin antibody.

(**C**) The doxycycline dose and time response growth MTT assay resulted in a reduction in TT-TRE NICD3 cell proliferation. (**D**) The doxycycline does not affect the proliferation of cells containing empty vector (TT-TRE) at any dose or time point indicating that NICD3 activity is necessary for TT cell growth reduction. Statistical significance was determined by repeated ANOVA followed by a protected Fisher's LSD for post hoc comparisons. (**E**) The degree of tumor cell growth inhibition (**2C**) is directly proportional to the amount of Notch3 protein present as assessed by Western blot after 6 day treatment with various concentrations of doxycycline (cells were retreated at days 2 and 4). All values are presented as a mean ±SD (n=4) *, P<0.05, ***, P<0.001.

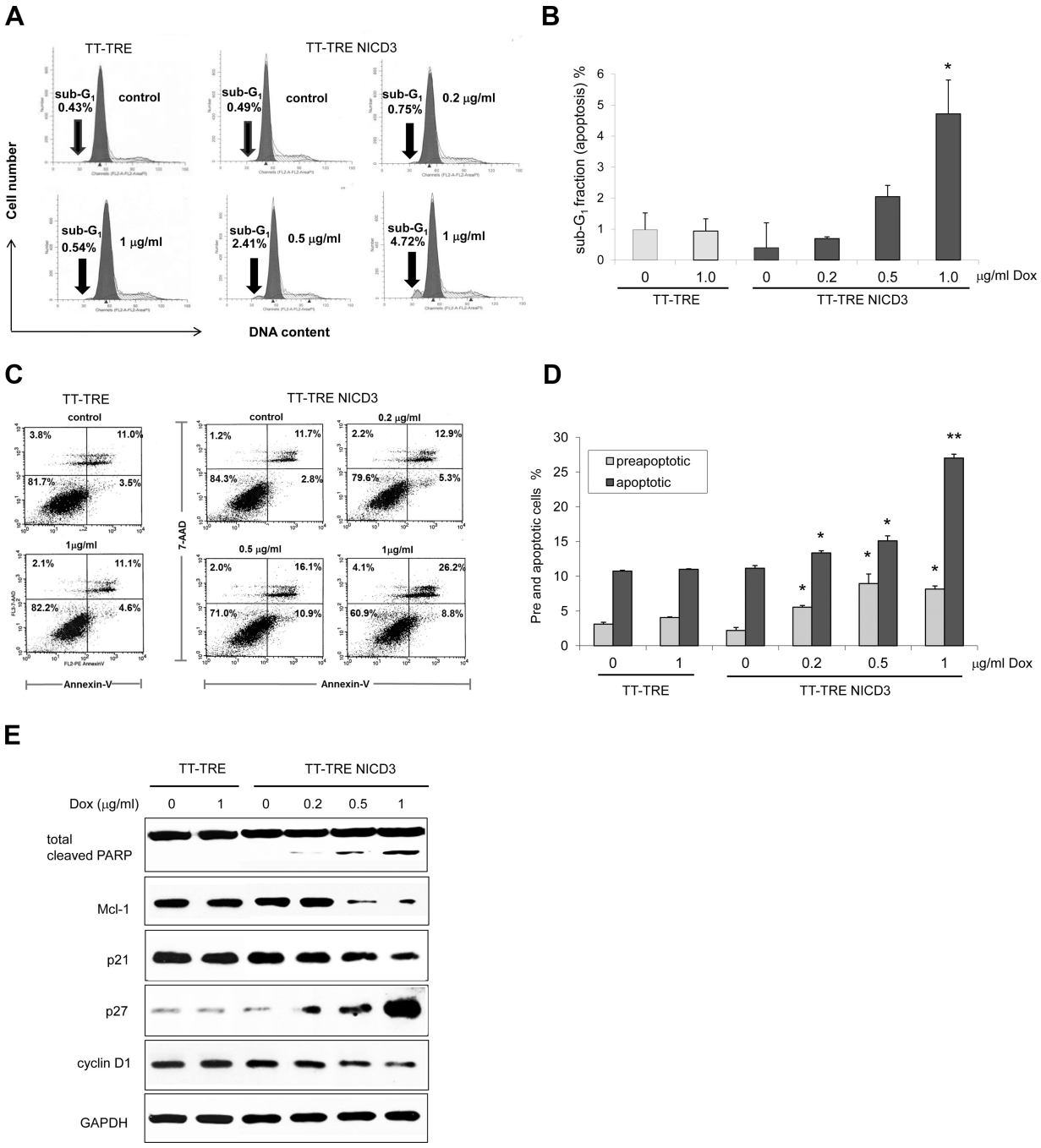

Figure 3. Active NICD3 suppresses MTC-TT cell growth by inducing apoptosis

(**A**) Conditional induction of NICD3 resulted in dose-dependent accumulation of sub- G_1 (i.e., sub-2N) DNA, assessed by flow cytometry analysis of PI stained cells. In contrast, no doxycycline effect was observed on the control vector cell line (TT-TRE). (**B**) Percentage denotes apoptotic cellular debris. Data from three independent experiments are summarized in the bar graph format and are shown as ±SEM. *, P<0.05. (**C**) The apoptosis was quantified by phoshatidylserine exposure using PE Annexin V/7AAD staining. Cells in the lower left quadrant indicate Annexin V negative/7-AAD negative: intact cells, lower right

quadrant indicate Annexin V-positive: early apoptotic cells, upper right quadrant indicate Annexin V-positive/7-AAD-positive: late apoptotic cells and necrotic cells in the upper left quadrant are positive only for 7-ADD staining. TT-TRE cells served as a negative control of apoptotic induction by doxycycline. (**D**) The bar graph represents pre- and apoptotic cells from three independent experiments which are shown as ± SEM. *, P<0.05, **, P<0.01. (**E**) Apoptosis was validated by Western blotting for the various apoptotic regulatory proteins.

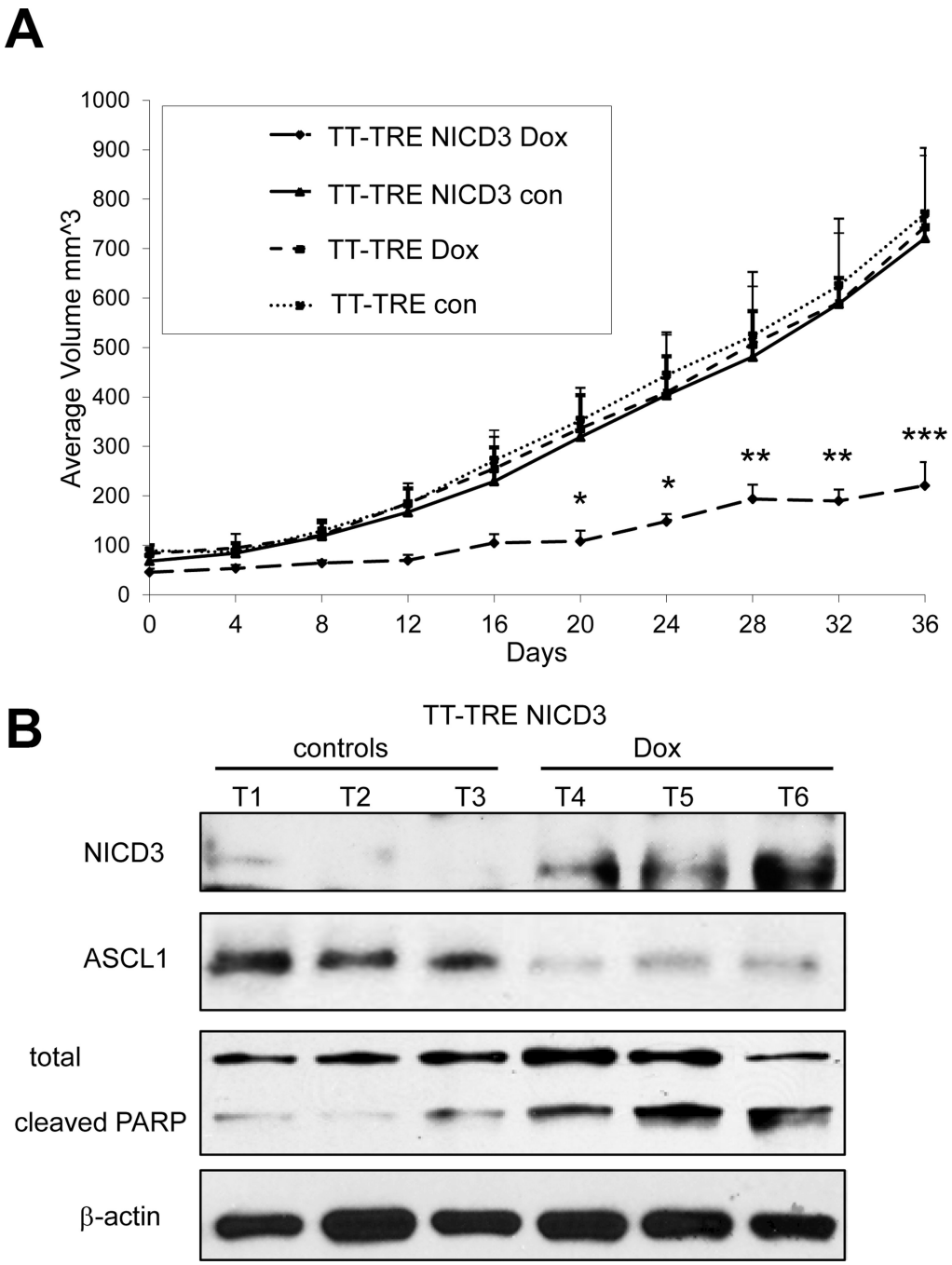

Figure 4. Expression of active Notch3 decreases MTC-TT cell growth *in vivo*

(**A**) Mice in the control groups (TT-TRE NICD3 con, TT-TRE dox and TT-TRE con) developed rapidly growing subcutaneous MTC tumors. In contrast, mice bearing doxycycline inducible TT-TRE NICD3 tumors exhibited significantly retarded tumor development. Overall longitudinal tumor volumes of 22 mice were evaluated across treatment groups at each of the ten time points using repeated ANOVA followed by a protected Fisher's LSD for post hoc comparisons. All analyses were conducted using SAS 9.3 (SAS Institute, Cary NC) software. Each data point represents the mean ±SD of five

(TT-TRE NICD3) or six (TT-TRE) animals. The significant difference in tumor volumes between NICD3 expressing xenografts (TT-TRE NICD3 dox) and tumors from the three control groups (TT-TRE NICD3 con, TT-TRE dox and TT-TRE con) was observed at day 20 of treatment (*, $P<0.05$), and increased with time of treatment (at days 28 and 32, **, P<0,01 and at day 36,***, $P<0.001$). (**B**) Western blot analysis of tumor tissue samples shows doxycycline induction of NICD3 in TT-TRE NICD3 xenografts, with concomitant decrease in the NE marker ASCL1, and cleavage of apoptotic marker PARP. β–actin was used as a loading control. TT-TRE NICD3 tumor bearing animals are represented by three tumor lysates from each treatment group.

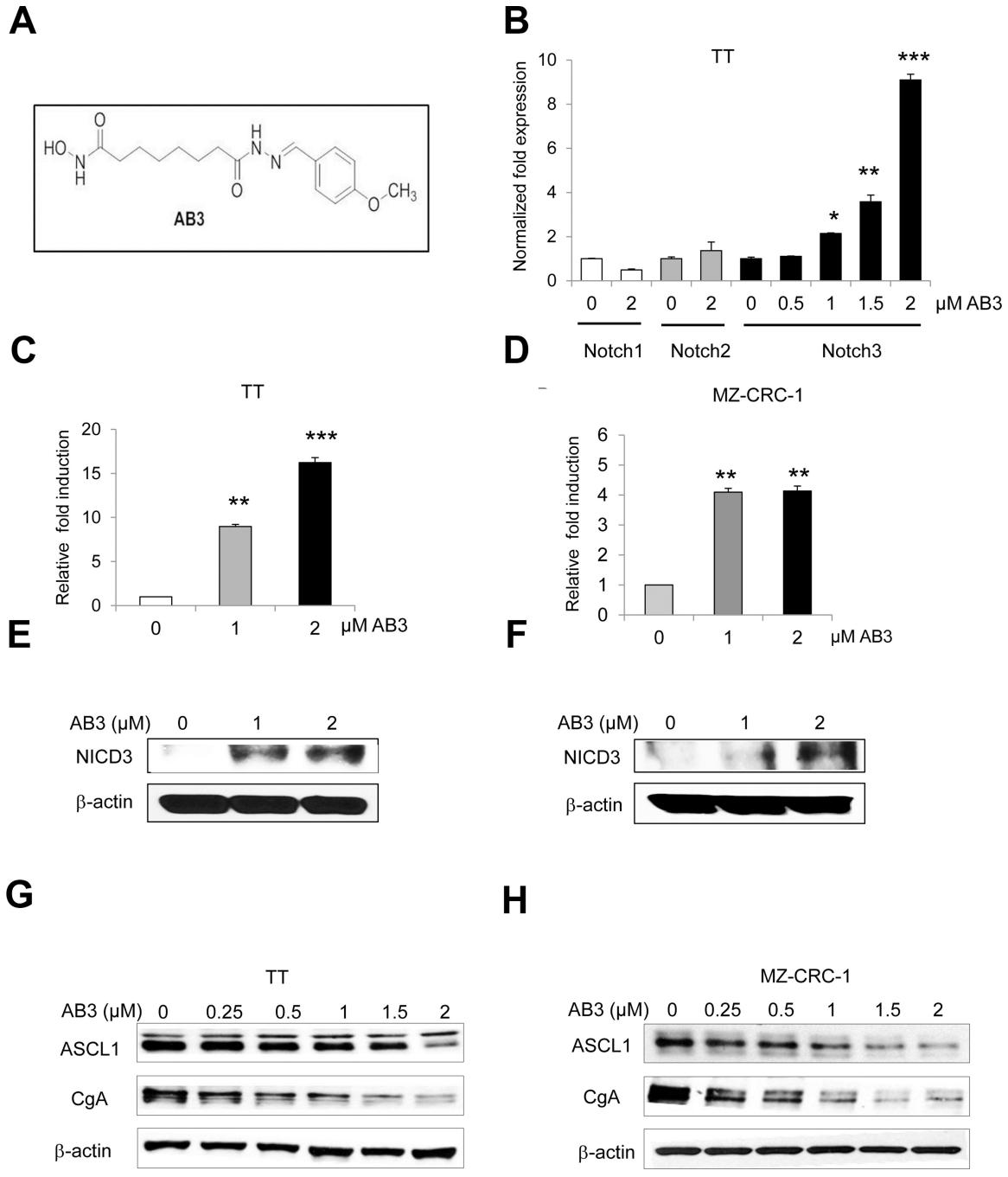

Figure 5. AB3 induces Notch3 signaling in MTC cell lines

(**A**) Chemical structure of HDAC inhibitor, AB3. (**B**) AB3 induced Notch3 in TT cells at the mRNA level in a dose–dependent manner, measured by qRT-PCR. Notch1 and Notch2 isoforms did not respond to AB3 treatment. (**C**) TT and (**D**) MZ-CRC-1 cells were transiently transfected with a luciferase construct containing four CBF1-binding sites (4 × CBF1- Luc) and treated with various concentrations of AB3 up to 48 hours. NICD3 function was assessed by the degree of NICD3–CBF1 binding measured by luciferase reporter assay. Luciferase values were normalized to β-galactosidase activity and are expressed as fold

increase relative to cells not treated with AB3. All values are presented as a mean ±SD (n=3). Western blot analysis of Notch3 intracellular domain (NICD3) in TT (**E**) and MZ-CRC-1 cells (**F**) treated with different concentrations of AB3 or vehicle control. Equal loading was confirmed with β–actin. 48 hours of AB3 treatment resulted in dose-dependent reduction in NE markers expression ASCL1 and CgA in TT (**G**) and MZ-CRC-1 (**H**) cell lines. *, $P<0.05$,**, $P<0.01$,***, $P<0.001$.

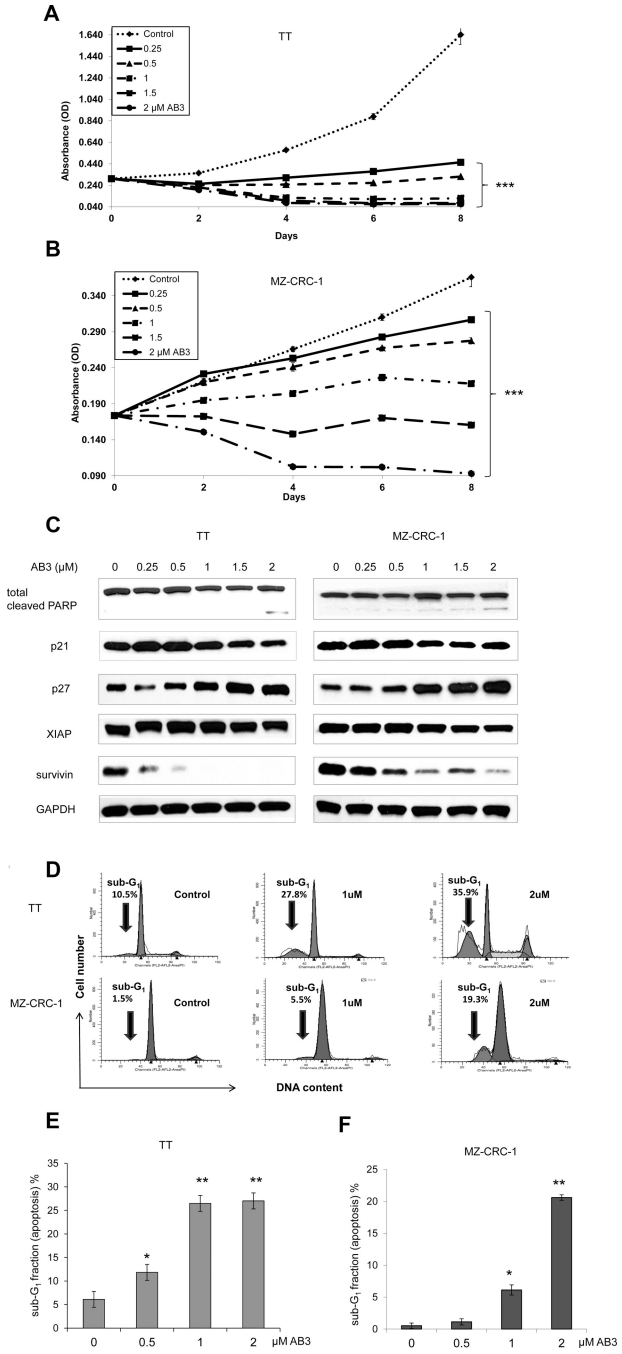

Figure 6. AB3 inhibits MTC cell line proliferation by inducing apoptosis

AB3 treatment reduced cell viability in a dose and time dependent manner in TT (**A**) and MZ-CRC-1 (**B**) cell lines, measured by MTT assay. (**C**) AB3 treatment resulted in changes in the various apoptotic regulatory proteins. (**D**) Apoptosis was validated by dose-dependent accumulation of sub-G_1 DNA, assessed through flow cytometry analysis of PI stained TT and MZ-CRC-1 cells. Percentage of sub-G_1 denotes apoptotic cellular debris of TT (**E**) and MZ-CRC-1 (**F**) cell lines summarized in bar graph format and are shown as ±SEM (n=3). *, P<0.05, **, P<0.01,***, P<0.001.

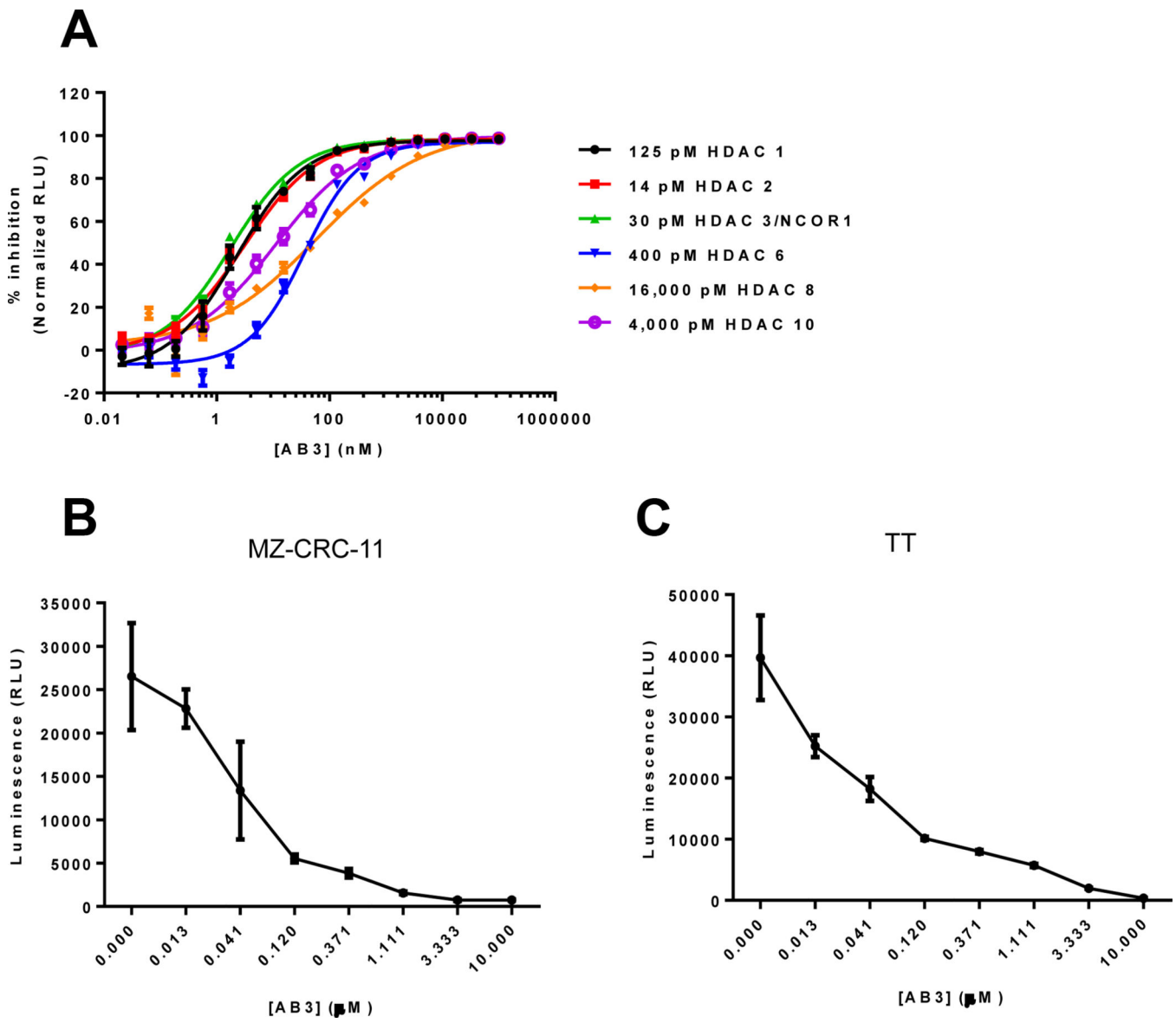

Figure 7. Activity and selectivity of AB3, a pharmacological inducer of Notch3

(**A**) Biochemical IC_{50} determination of the HDAC inhibitor, AB3, using purified human recombinant HDAC's and the HDAC-Glo™ I/II Assay. Each data point represents n = 4 replicates and error bars are +/− standard deviation. Curve-fits to determine IC_{50} values (sigmoidal dose response, variable slope) were generated using GraphPad Prism (version 6.03, GraphPad Software, Inc). (**B**) Inhibition of HDAC activity in the MZ-CRC-1 and TT (**C**) cell lines using the HDAC inhibitor, AB3, and the HDAC-Glo™ I/II Assay. Each data point represents n = 3 replicates and error bars are +/− SEM. The graphs were generated using GraphPad Prism (version 6.03, GraphPad Software, Inc).

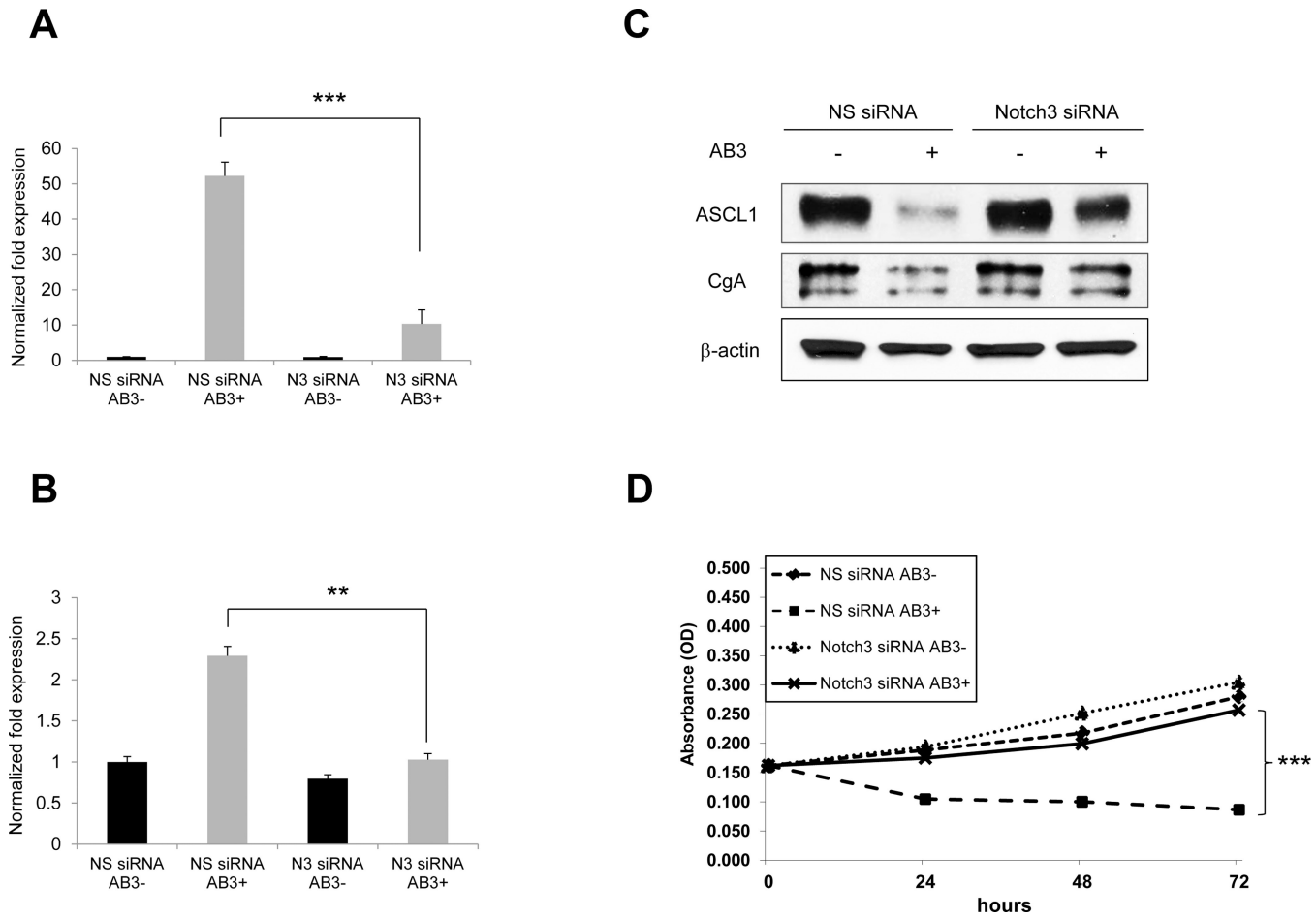

Figure 8. The inhibitory effects of AB3 on the neuroendocrine phenotype of MTC depend on Notch3 activation

TT cells were transiently transfected with siRNA against Notch3 or a nonspecific siRNA and then treated with AB3. QRT-PCR expression analysis demonstrates that Notch3 targeted siRNA were capable to significantly reduce AB3-activated Notch3 (**A**) and downstream HES1 message levels (**B**) following 48h of AB3 treatment. (**C**) Western blot analysis showed that AB3-induced abrogation of neuroendocrine malignancy markers ASCL1 and Chromogranin A was markedly recovered when Notch3 levels were concomitantly silenced. (**D**) 72h silencing of Notch3 in the presence of AB3 restored proliferation of TT cells. All values are presented as a mean ±SD (n=3). **, P<0.01,***, P<0.001.

Table:1

IC_{50} values (nM) of AB3 listed against the indicated purified human recombinant HDAC isoform.

HDAC isoform	AB3 IC_{50} (nM)
HDAC 1	**2.28**
HDAC 2	**3.12**
HDAC 3/NCOR1	**1.82**
HDAC 6	**35.80**
HDAC 8	**60.32**
HDAC 10	**11.05**